PCCP

Accepted Manuscript

ROYAL SOCIETY OF CHEMISTRY

www.rsc.org/pccp

Cite this: DOI: 10.1039/c0xx00000x

www.rsc.org/xxxxxx

ARTICLE TYPE

Enhanced photoluminescence and photoactivity from Plasmon sensitized nSiNWs/TiO_2 Heterostructures

Sandeep G. Yenchalwar[a,b], Vedi Kuyil Azhagan[a], Manjusha V. Shelke*[a,b,c]

Received (in XXX, XXX) Xth XXXXXXXXX 20XX, Accepted Xth XXXXXXXXX 20XX
DOI: 10.1039/b000000x

Light sensitive wide band gap radial heterojunction between TiO_2 and nSiNWs, sensitized by gold nanoparticles is reported here. Surface plasmon of AuNPs influences the optical and photocurrent properties of the heterojunction considerably. Improvement in the band gap emission of TiO_2 has been found at the expense of defect radiation. Excitation of AuNPs deposited on nSiNWs/TiO_2 by light irradiation shows wavelength dependent photocurrent due to increased photoactivity of the heterojunction.

Light detection and photocurrent generation from the excitation of surface plasmon on the metal nanoparticles' surface is a recent concept**.** There has been a profound surge of interest in exploiting the collective oscillations of the conduction electrons of metal as a powerful way to incorporate into nanoscience and nanotechnology. Metal nanoparticles exhibit localized surface plasmon resonance (LSPRs) by interaction of visible light photons with the valence electrons on the metal surface. At a resonance frequency of metal nanoparticles the strongest optical interaction occurs being a function of the size, shape, type of metals as well as the local dielectric environment [1, 2]. The large resonant scattering cross sections of metal nanostructures offer the potential to scatter the light strongly while LSPs can guide and confine light flux in nanoscale dimensions [3]. The LSPs decay radiatively by scattering or non-radiatively resulting in energy absorption [4]. These tunable properties of metal nanoparticles can be used in variety of applications from non-linear optics, photovoltaics to sensing [5-7].

Due to versatile properties and easy, controllable synthesis Silicon nanowires (SiNWs) are important candidates for optoelectronic devices, solar cells [8, 9]. One dimensional SiNWs arrays offer increased surface area, enhanced light absorption, reduced charge recombination. Oxides with wide band gap and high dielectric constant, commonly called as k-oxides are of great interest in the electronic industry. TiO_2 is a remarkable semiconductor material with a large band gap (3.0-3.2 eV), chemically inert, high photo-conversion efficiency and good photo-stability [10, 11]. Although, Si is more efficient it corrodes in water and large band gap of TiO_2 restricts its applications in certain requirements e.g. water splitting in the visible part of the spectrum. Semiconductor heterojunction are being studied to overcome these shortcomings. The performance of the functional device in water splitting application is based on the heterojunctions formed between TiO_2 and Silicon. Such heterojunctions allow effective separation and utilization of charge carriers (e^-/h^+) by increased absorption of the light. The band bending near the junction of nSiNWs/TiO_2 for photo-oxidative properties of the hybrid in photoelectrochemical cell has been studied where it has been observed that photocurrent increases due to enhanced charge separation and minimum recombination [12]. Photocatalytic degradation of phenol on the electrode with n-n and p-n heterojunctions has been observed between SiNWs and TiO_2 [13]. Semiconductor/metal composites are highly appreciated for their visible light sensitivity because of plasmonic antenna effect of metal nanoparticles extending the absorption range of wide band gap semiconductors. Such hybrid nanomaterials show enhanced physical properties such as low reflection, high absorption, dielectric strength etc.

In this work, we demonstrate the effect of gold nanoparticles surface plasmon on SiNWs/TiO_2 heterojunctions. These hybrids show enhanced optical absorption, emission and photocurrent generation. Plasmonic sensitization enhances self trapped exciton emission and oxygen vacancy radiative recombination emission properties of TiO_2. Light emitting diodes (LEDs) are used as a source of light for photocurrent measurements. Enhanced photocurrent is achieved by decorating AuNPs on the surface of nSiNWs/ TiO_2 heterojunctions due to plasmonic charge carrier generation.

Result and Discussion:

As prepared heterojunction materials are characterized by SEM, **Figure 1 a** and **b** shows the images of vertical SiNWs of approximately 3µm in length and 100 nm in diameter. It can be seen in **Figure 1 b** that the individual Si nanowires are uniformly covered with the TiO_2 layer. **Figure 1c, d** show the HR-TEM images of same SiNWs/ TiO_2 sample, thickness of the TiO_2 layer is ~20 nm with 8.6 nm (~ 9 nm) sized gold nanoparticles on its surface suggesting the effectiveness of the process utilized herein for the synthesis of the hybrids. The nanoparticles are found to be buried in the TiO_2 matrix because during synthesis samples were soaked in gold salt solution where Au (III) ions may have percolated through the TiO_2 layer.

Figure 2 a, is the typical XRD pattern of gold nanoparticle decorated radial heterojunction of SiNWs/TiO_2. The peaks at 2θ = 32.2 (100) and 69.3 (400) corresponds to highly crystalline

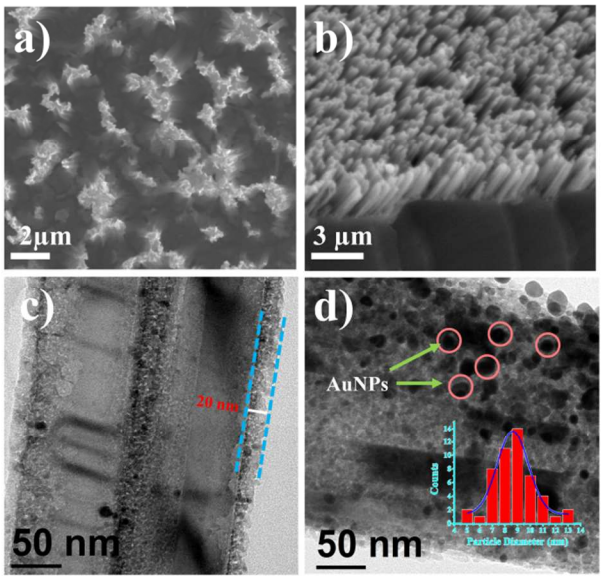

Figure 1. a) Top view, b) Cross section (tilt at 45°) SEM views of asprepared nSiNWs/TiO_2 heterojunction while c), d) are the HRTEM images of the TiO_2 coated nSiNWs and after gold nanoparticle deposition respectively.

nature of SiNWs. The peaks appearing at 25.4 (101), and 75.3 (215) belongs to the crystalline, anatase phase of the TiO_2 [JCPDS No. 841285]. New peaks at 38.2 and 44.4 represent (100) and (200) orientations of face centered cubic symmetry of gold nanoparticles [JCPDS No. 040784].

The diffuse reflectance spectra (**Figure 2 b**) were recorded for the pristine SiNWs, TiO_2 coated SiNWs and Au nanoparticles deposited SiNWs/TiO_2 samples. All samples show low reflectance over the spectral range of 300-800 nm than the Silicon. It reveals increased light harvesting capability of heterojunctions than the pristine SiNWs. TiO_2 thin layer on the SiNWs acts as a surface passivating layer as well as antireflection coating improving the absorbance by multiple internal reflections.

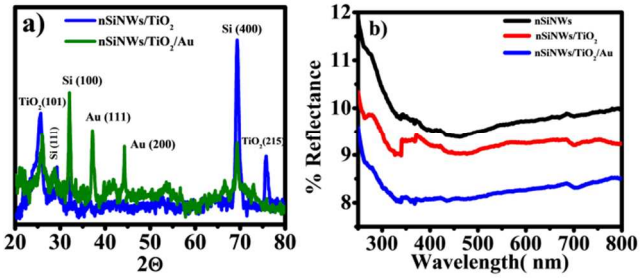

Figure 2. a) X-Ray Diffraction pattern showing anatase form of the thin TiO_2 overlayer alongwith typical gold lattice planes. b) Comparative Diffuse Reflectance Spectra of the as prepared samples.

The heterojunction can utilize both visible and UV-light of the solar spectrum which remarkably enhances its properties towards application. The TiO_2 coated SiNWs samples show ~ 8% reflectance over the entire visible range after gold nanoparticle embedding in the TiO_2 matrix including the interband transition of SiNWs and TiO_2. Also, an increase in absorption in the range of 450-550 nm is due to surface plasmon of gold nanoparticles. The mechanisms such as i) change in the refractive index of the metal oxide (here TiO_2) due to embedded gold nanoparticle, ii) change in the effective electron density of the AuNPs can be responsible for the broad nature of the peak. AuNPs deposition on the TiO_2 overlayer further causes enhancement in light absorption. This is possibly due to LSPRs caused by the light interactions which increases the scattering ability of AuNPs in the medium of higher refractive index leading to more photon absorption [14].

Raman scattering is a sensitive technique to probe lattice microstructures and vibrations. Raman spectra (**Figure 3 a**) display the crystallinity of SiNWs and TiO_2 moreover, it suggests the strain induced by the thin layer coating of TiO_2 on SiNWs and disordered or rough surface of SiNWs. The sharp peak at 145.60 cm^{-1} and 636.96 cm^{-1} belongs to optical vibration E_g modes in anatase TiO_2 [15]. The peak at 520.13 cm^{-1} which is characteristic of crystalline silicon arises from the scattering of incident light with the first order longitudinal and transversal optical phonon (LTO) in the diamond structures of SiNWs. While peak at 303.86 cm^{-1} is the second order transverse acoustic phonon (2TA) contribution which is significantly appears in the spectra [16, 17]. The selection rule does not allow this band to appear in normal crystalline Si, which is broken in disordered material. The band for E_g mode further gets enhanced after AuNPs deposition and a little shift of 1 cm^{-1} is observed. The broad band centered at 960.1 cm^{-1} is related to second order transversal optical phonons (2TO) in silicon, also suggests the strong interaction between the titanium thin films with the silicon surface. The peak at 855.8 cm^{-1} could be ascribed to Ti-O-Ti stretch indicating the 2D-type connectivity [18].

Solid state PL spectroscopy was used to understand the presence of defects and recombination ability of charge carriers. Room temperature photoluminescence spectra have been plotted in the **Figure 3 b.** The as prepared samples were excited at the band edge absorption of the TiO_2 i.e. 340 nm. Both show multi-emission peaks which have been de-convoluted using Gaussian fitting in order to understand their peak position and nature. For the semiconductors such as TiO_2, ZnO on excitation with the photon energy equal to or higher than their band gap, electrons can be transferred from valence band to conduction band generating excitons which after recombining emit radiation approximately equal to its band gap. But, this is not always true, since presence of defects such as oxygen deficiencies, impurities or metal doping creates the sub-energy levels that can capture the electrons, resulting into emission of less energy photons than the band gap. The oxygen related defects in TiO2 are intrinsic and particularly important as it give rise to intermediate energy levels within the band gap. As a consequence many recombination centers are introduced for electron-hole pairs.

In the absence of gold nanoparticles, TiO_2 shows (**Figure 3 c**) PL peaks at 415 nm, 451 nm and 503 nm belongs to self trapped excitons (STEs), oxygen vacancies with two electrons (F-center or $V_O^{\bullet\bullet}$) and oxygen vacancies with one electron ($V_O^{\bullet}$) respectively. After gold nanoparticle deposition (**Figure 3 d**) new peaks appeared at 403 nm, 433 nm and 458 nm. All these peaks confirm the anatase type of TiO_2 thin layer formed on the SiNWs. The PL of anatase TiO_2 arises from three different physical origins namely radiative recombination of self trapped excitons, oxygen vacancies (OVs) and surface states [19] in the defect state

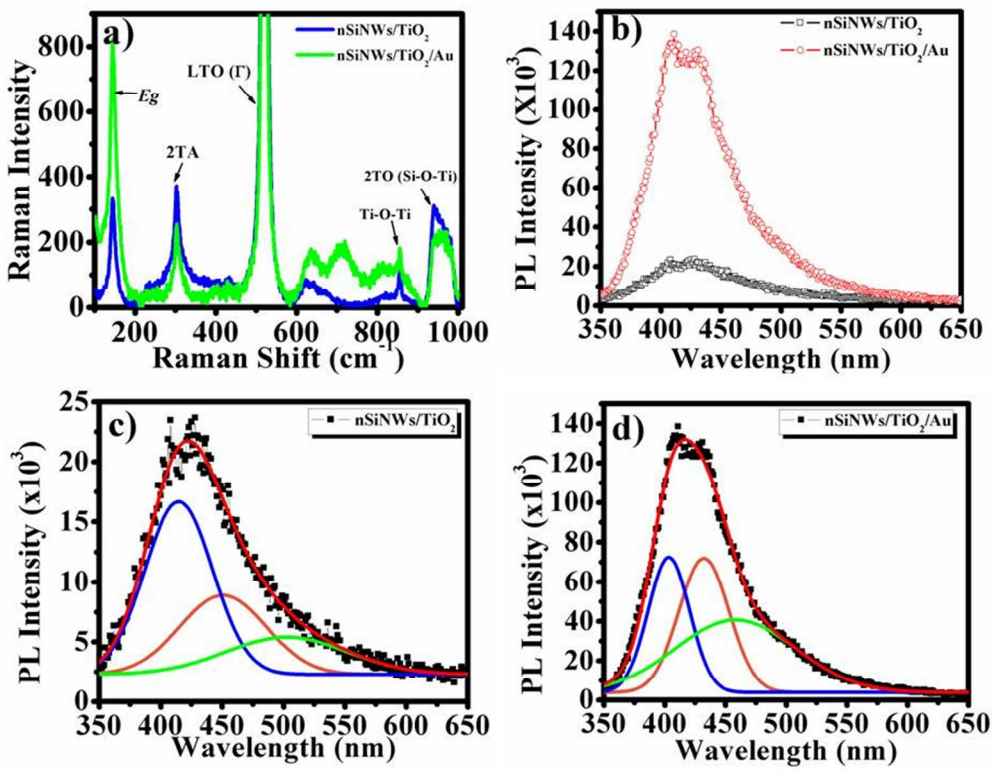

Figure 3. a) Micro-Raman spectra before and after AuNPs deposition on nSiNWs/TiO_2 heterojunction indicating typical anatase peak of TiO_2 with 1st and 2nd order Silicon peaks. b) Room temperature Photoluminescence of the heterojunctions. c), d) represents the Gaussian fitted PL peaks of the as prepared samples before and after AuNPs deposition.

within the band gap. It has been reported that oxygen vacancies in metal oxides behave as a deep trap states which enhances the recombination of charge carriers and shallow trap states promotes diffusion of carriers to the surface [20, 21].

The mechanisms for the PL in TiO_2 can be described by the following processes [19].

$$TiO_2 \xrightarrow{h\nu} TiO_2\,(e^- + h^+) \Longrightarrow e^-_{CB} + h^+_{VB}$$

$$V_O^{\,0} + e^-_{CB} \Longrightarrow V_O \quad \text{(shallow state trapped electrons)}$$

$$V_O + h^+_{VB} \Longrightarrow V_O^{\,0} + h\nu \quad \text{(radiative recombination)}$$

Where, $V_O^{\,0}$ is a Kroger notation for the ionized oxygen vacancy level.

The conduction and valence band edges for titanium oxide lies at ~ 4.26 eV and ~7.46 eV with respect to the vacuum considering the anatase TiO_2 band gap of 3.2 eV[22]. The shallow traps belonging to oxygen vacancies were established at 0.51 eV [19] and 0.8 eV [23] below the conduction band. The peaks viz. 451 nm and 503 nm as obtained in the **figure 3 c** are nearly coincident with these OVs level.

The electrons excited from the VB of the TiO_2 cannot reach to the CB of TiO_2 instead they are captured by the oxygen vacancies via non-radiative process and then recombine with the holes in VB accompanying radiative emission in visible region corresponding to the peak 415 nm. The blue shift of 12 nm in the band edge luminescence is observed for the gold deposited samples suggesting trapping of electrons in the energy level just below the CB of TiO_2. It also emphasizes the strong interfacial interaction between TiO_2 and gold nanoparticles. The emission at 432 nm corresponds to self trapped exciton (STE) which has been suggested to occur due to oxygen vacancies created by metal doping (here by Au metal) [24, 25]. Considerably increased intensity of the shallow trap states after gold nanoparticles deposition infers increased radiative recombination at this level. The photoluminescence of the heterojunction on gold deposition shows 5 times enhancement after integrating the emission signals of TiO_2. This suggests that the rate of semiconductor emission in a gold nanoparticle deposited heterojunction system, which is a function of concentration of electron-hole pairs in the semiconductor, is larger than the only heterojunction system. It can be explained only by the involvement of AuNPs SPR which increases the rate of electron-hole pair formation in the semiconductor due to near-field effect. The photoexcited plasmonic AuNPs efficiently scatter resonant photons increasing the average photon path-length in the TiO_2 layer ultimately results into enhanced rate of exciton formation. More precisely, the defect emission energy (503 nm) is close to SPR of gold nanoparticles as per the DRS spectra. This energy is absorbed by the gold nanoparticles generating energetic electrons (hot electrons) in the high energy state within the Fermi level which could be transferred from gold nanoparticles into the conduction band of the TiO_2. Later, by combining with the holes in the VB of the TiO_2 they relax by emitting energetic photons and results in

increase in the intensity of the other emission band of TiO_2 [26, 27].

To investigate the effect of the increased absorption and PL due to gold nanoparticles on photocurrent, we carried out photocurrent measurements. Spectrally resolved photoelectrochemical behavior of the samples was studied in neutral medium using Na_2SO_4 solution under LED light illumination. Both electrodes were photoactive to the LED light irradiation. **Figure 4 A**, shows the linear sweep voltammograms before and after gold nanoparticle deposition on heterojunction, recorded in the potential range between -1 to +2 V Vs Ag/AgCl as a reference electrode in dark and under white light illumination with a scan rate of 100 mV s^{-1}. Both the samples show pronounced photocurrent than the dark current, but substantially higher for gold nanoparticles deposited samples as evident from the graph. The dependence of photocurrent as a function of time of illumination at applied potential (0.5 V Vs Ag/AgCl) has been shown in the **Figure 4 B**.

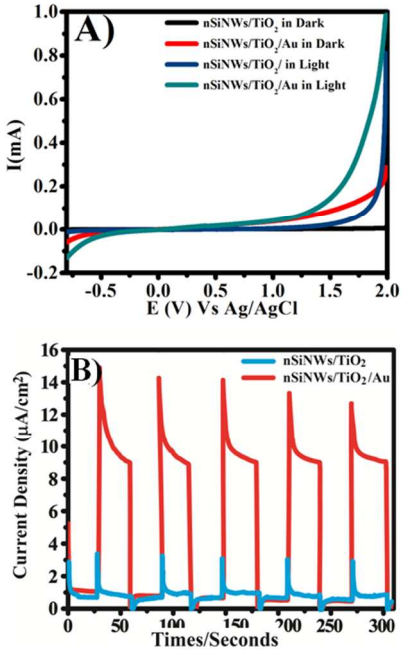

Figure 4. A) Linear sweep voltammograms (LSVs) and B) Transient photocurrent of the nSiNWs/TiO_2 and nSiNWs/TiO_2/Au samples under dark and white light illumination under the bias of 0.5 V Vs Ag/AgCl. The gold deposited nSiNWs/TiO2 heterojunction shows the highest photocurrent due to increased visible light absorption.

The SiNWs/TiO_2 heterojunction shows maximum photocurrent of 0.33 μA cm^{-2} in the white light illumination due to enhanced absorption of the visible light than the SiNWs and favorable band alignment for the possible photoexcited electron transfer. Photoelectrodes with AuNPs show approximately 25 times enhancement in the photocurrent (~ 8.4 μA cm^{-2}). This increment in the current can be attributed to the possible role of the gold nanoparticles as it enhances the other physical properties of the heterojunction as discussed above. In order to establish a role of gold nanoparticles in the photocurrent enhancement, a wavelength dependent study has been done and presented in the **Figure 5 A** and **B**. When irradiated with the Green LED light (central wavelength at 530 nm, total power output~ 22.3 mW cm^{-2}) with a incident power of 11.2 mW on the prescribed area of the electrode i.e. 0.5 cm x 0.5 cm, it gives highest current than the other wavelengths.

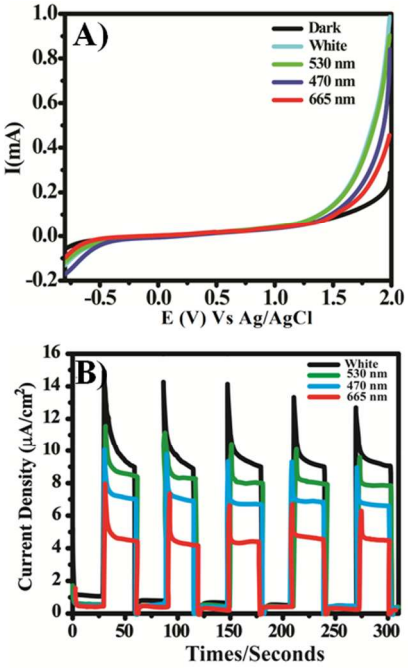

Figure 5. A) LSVs and B) Wavelength dependent photoresponse of the nSiNWs/TiO_2/Au. All measurements were carried out giving bias of 0.5 V Vs Ag/AgCl in 1 M Na_2SO_4 as an electrolyte .

The gold deposited on the heterojunction has a maximum absorbance in the region of 400-550 nm which is due to combine effect of SPR and dielectric strength of the TiO_2. Therefore, it is reasonable to accept that the photocurrent response for 470 nm (~ 6.43 μA cm^{-2}) and 530 nm (~ 7.8 μA cm^{-2}) is because of the spectral overlap of the energy levels of the SPR of gold nanoparticles and TiO_2. The photon energy (530 nm) is particularly absorbed by the gold nanoparticles than the high energetic photons (470 nm) and hence the maximum photocurrent is observed for the green light irradiation. The absorbance of the gold deposited samples extends in the entire visible region, hence it should be able to convert incident photons of 665 nm wavelength too which results into the higher photocurrent (~ 4.14 μA cm^{-2}) at this wavelength.

To produce photocurrent from the AuNPs deposited nSiNWs/TiO_2, the electrons and holes must have to be transferred across the heterojunction.

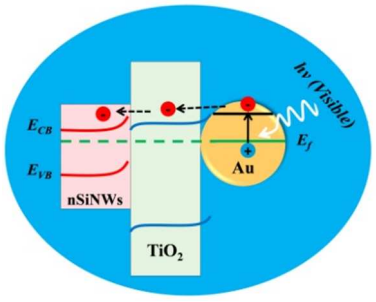

Scheme 1. Simplified illustration for the band energies and possible charge transfer from gold nanoparticle SPR level into the conduction band of TiO2 under visible light illumination.

A barrier of 1.1 eV exists between AuNPs-TiO_2 interface because of the difference in work function of gold (~ 5 eV) and electron affinity of TiO_2 (~ 3.9 eV) [28] which has to be overcome by the electrons so as to contribute in the current. As the present study suggest the increase in the photocurrent on visible light irradiation indicating that these electrons have enough energy to cross the Schottky barrier. Also, SPR on gold can be stimulated by the defect emission (~2.5 eV) energy transfer. The excited SPRs might be responsible for the electron tunneling from gold to TiO_2 conduction band. As a result electron density increases in the conduction band of TiO_2, leading to higher recombination rate of electron-hole that enhances the PL properties of TiO_2. All these facts suggest the synergistic effect between TiO_2 emission and gold SPR involvement in the enhanced photoactivity of the heterojunction.

Conclusions

A simple method has been presented for the synthesis of heterojunction alongwith improved and new properties of such heterojunction by depositing gold nanoparticles. The influence of SPR of gold nanoparticles on the optical and photocurrent properties of the nSiNWs/TiO_2 heterojunction has been investigated. Such gold plasmon sensitized SiNWs/TiO2 exhibits broadband visible light absorbance and photoresponse with a peculiar wavelengths matching at the SPR and interband transitions. The enhanced absorption, enhanced rate of hole-electron formation, electric field amplification and simultaneous plasmonic energy transfer to the semiconductor is attributed to the increased response towards the multiwavelength photoconductivity of the heterojunction. The addition of noble metal nanoparticles on the semiconductors or semiconductor heterojunction can be effectively used in the preparation of highly efficient optoelectronic devices.

† Electronic Supplementary Information (ESI) available: [Experimental methods, EDAX analysis spectum]. See DOI: 10.1039/b000000x/

Notes

[a] Physical and Materials Chemistry Division, CSIR-National Chemical Laboratory,Pune-411008, MH, India
[b] Academy of Scientific and Innovative Research (AcSIR), AnusandhanBhawan, 2 Rafi Marg, New Delhi-110001
[c] CSIR-Network Institute of Solar Energy, CSIR-National Chemical Laboratory, Pune-411008, MH, India

Acknowledgment

SGY acknowledges research fellowship from UGC. This work is supported by the Council of Scientific and Industrial Research (CSIR), India through TAPSUN program.

References

1. K. L. Kelly, E. Coronado, L. L. Zhao and G. C. Schatz, *J. Phys. Chem. B*, 2003, **107**, 668.
2. L. Gunnarsson, *J. Phys. Chem. B* 2005, **109**, 1079.
3. J. A. Schuller, E. S. Barnard, W. Cai, Y. C. Jun, J. S. White and M. L. Brongersma, *Nature Mater.*, 2010, **9**, 193.
4. M. Kauranen and A. V. Zayats, *Nature Photon*, 2012, **6**, 737.
5. H. A. Atwater and A. Polman, *Nature Mater.*, 2010, **9**, 205.
6. S. Nie and S. R. Emory, *Science*, 1997, **275**, 1102.
7. S. Kühn, U. Håkanson, L. Rogobete and V. Sandoghdar, *Phys. Rev. Lett.* , 2006, **97**, 017402.
8. B. Tian, X. Zheng, T. J. Kempa, Y. Fang, N. Yu, G. Yu, J. Huang and C. M. Lieber, *Nature Mater.*, 2007, **449**, 885.
9. I. Hochbaum, R. Chen, R. D. Delgado, W. Liang, E. C. Garnett, M. Najarian, A. Majumdar and P. Yang, *Nature Mater.*, 2008, **451**, 163.
10. X. Chen and S. S. Mao, *Chem. Rev.* , 2007, **107**, 2891.
11. R. Asahi, T. Morikawa, T. Ohwaki, K. Aoki and Y. Taga, *Science*, 2001, **293**, 269.
12. Y. J. Hwang, A. Boukai and P. Yang, *Nano Lett.*, 2009, **9**.
13. H. Yu, X. Li, X. Quan, S. Chen and Y. Zhang, *Environ. Sci. Technol.*, 2009, **43**, 7849.
14. K. R. Catchpole and A. Polman, *Opt. Express*, 2008, **16**, 21793.
15. D. Bersani, P. P. Lottici and X.-Z. Ding, *Appl. Phys. Lett.*, 1998, **72**, 73.
16. R. Wang, G. Zhou, Y. Liu, S. Pan, H. Zhang, D. Yu and Z. Zhang, *Phys. Rev. B*, 2000, **61** 16827.
17. B. Li, D. Yu and S. L. Zhang, *Phys. Rev. B*, 1999, **59**, 1645.
18. M. Ferna´ndez-Garcı´a, X. Wang, C. Belver, J. C. Hanson and J. A. Rodriguez, *J. Phys. Chem. C*, 2007, **111**, 674.
19. N. Serpone, D. Lawless and R. Khairutdinovt, *J. Phys. Chem.*, 1995, **99**, 16646.
20. Y. Lei, L. D. Zhang, G. W. Meng, G. H. Li and X. Y. Zhang, *Appl. Phys. Lett.*, 2001, **78**, 1125.
21. G. Mattioli, F. Filippone, P. Alippi and A. M. Bonapasta, *Phys Rev B*, 2008 **78**, 241201.
22. I. Chung, B. Lee, J. He, R. P. H. Chang and M. G. Kanatzidis, *Nature.* 2012, **485**, 486.
23. L. V. Saraf, S. I. Patil, S. B. Ogale, S. R. Sainkar and S. T. Kshirsager, *Int. J. Mod. Phys. B*, 1998, **12**, 2635.
24. K. Iijima, M. Goto, S. Enomoto, H. Kunugita, K. Ema, M. Tsukamoto, N. Ichikawa and H. Sakama, *J Lumin*, 2008, **128**, 911.
25. B. Choudhury, M. Dey and A. Choudhury, *Appl Nanosci*, 2013.
26. C. W. Cheng, E. J. Sie, B. Liu, C. H. A. Huan, T. C. Sum, H. D. Sun and H. J. Fan, *Appl. Phys. Lett.*, 2010, **96**, 071107.
27. H. Y. Lin, C. L. Cheng, Y. Y. Chou, L. L. Huang and Y. F. Chen, *Optics Express*, 2006, **14**, 2372.
28. G. Rothenberger, D. Fitzmaurice and M. Gratzel, *J. Phys. Chem.*, 1992, **96**, 5983.

Table Of Content:

Radial heterostructures of nSiNWs/TiO_2 exhibits improved optical properties due to surface plasmon of gold nanoparticles where band gap emission increases at the expense of defect radiation and higher photocurrent as a result of near field effect combined with subsequent plasmonic energy transfer.